



Study on the design and cutting performance of stepped bi-directional milling cutters for hole making of CFRP

Chen Tao¹ · Li Rui¹ · Xiang Jiupeng¹ · Gao Weijie¹ · Wang Yongsheng¹

Received: 7 February 2020 / Accepted: 7 May 2020 / Published online: 16 June 2020
© Springer-Verlag London Ltd., part of Springer Nature 2020

Abstract

During hole making of carbon fiber reinforced plastic (CFRP) by helical milling, the tool wear is a main factor in machined surface damage, being unable to guarantee machining quality and accuracy, and restricting the improvement of hole making efficiency. In order to prolong the service life of cutters, this paper has carried out the research into the design, manufacture, and cutting performance of stepped bi-directional milling cutters, combining with hole making of CFRP by bi-directional helical milling. By the method of differential geometry, the geometric model of the profile shape and the mathematical model of the helical edge are established of the stepped bi-directional milling cutter. Additionally, based on the transformation matrix between grinding wheel and workpiece coordinates of any point, the track equation of grinding wheel is derived from grinding the side edge helical groove of the stepped bi-directional milling cutter. What is more, the grinding process and accuracy are measured about the designed stepped bi-directional milling cutter. The experiment of CFRP holes made by bi-directional helical milling is designed, and the experimental results show that the axial cutting force of stepped bi-directional milling cutters is smaller and fluctuates more gently than that of symmetrical bi-directional milling cutters in the backward milling. Especially, the former has better distributed and slower flank wear on the backward cutting edge, and better machining quality than the latter.

Keywords Bi-directional helical milling · Cutting performance · Milling cutter design · Milling cutter manufacture · Stepped bi-directional milling cutter

1 Introduction

Compared with the conventional drilling technology, the helical milling technology—a new hole making technology—can greatly reduce the axial cutting force, effectively avoiding some defects such as delamination and tearing in hole making of CFRP [1, 2]. The helical milling technology shows great machining performance in processing aerospace composites. However, in machining composites by helical milling, the tool wear can cause some prominent problems of workpiece surface damage such as burrs and tearing, and there are still difficulties to guarantee machining quality and accuracy, thus restricting the improvement of hole making efficiency [3, 4]. Therefore, in speeding up popularization and application of

the helical milling technology for machining composites, it is urgent to prolong tool life by improving machining technology and designing new types of milling cutters.

Liu et al. [5] analyzed the kinematic characteristics of helical milling specialized tools by introducing the chip-splitting principle and designed a specialized cutter for helical milling with distributed multi-point front cutting edge by the method of optimizing end edge parameters. Chen et al. [6] presented a special mathematical model for S-shaped edge curve. The model overcame some shortcomings of traditional modeling method such as poor adaptability and complicated computation, and verified its own correctness by simulation. Based on the actual hole making by helical milling, Tian et al. [7] established a mathematical model of the relationship amongst tool structure, cutting area, and cutting depth, and proved itself by using numerical simulation. Ren et al. [8] proposed a new grinding method for milling helical grooves by means of analytic geometry and envelope theory, and verified its effectiveness by the numerical simulation and machining experiments. Through the machining technology of grinding helical grooves with five-axis CNC grinder, Wang et al. [9] deduced

✉ Chen Tao
dotnetchen@163.com

¹ School of Mechanical and Power Engineering, Harbin University of Science and Technology, Harbin 150080, China

the relational equation of grinding wheel's position and machined flute parameters, and presented a grinding method giving consideration to the interference and geometric anomaly in grinding helical grooves. Starting with the geometric constraints of grinding helical grooves, Nguyen et al. [10] analyzed the singular points in grinding by combining the engaging state of grinding wheel and workpiece, and proposed a novel mathematical model for determining the wheel location. An et al. [11] conducted an in-depth study on the formation mechanism of machined surface defects at the micro level, and analyzed the fracture mechanism of carbon fibers and its effects on machined surface morphology at various fiber orientation angles in the process of CFRP cutting. Gökhan et al. [12] determined the optimum cutting parameters and drill geometry for minimizing damage factor under dry machining conditions through Taguchi orthogonal experiment. Ömer et al. [13] used artificial neural network (ANN) models with five learning algorithms to study the damage factor in milling GFRP composite material, and found that the damage factor varied according to the change of cutting speed, feed rate, cutting depth, etc. Qi et al. [14] used the finite element method to analyze the cutting force in drilling CFRP and presented a mechanical model for delamination of CFRP. Ventura et al. [15] analyzed the relationship amongst tool contact angle, cut depth, and cutting force in helical milling, and established a prediction model of cutting force. Using analysis of variance and response surface methodology, Norbert et al. [16] analyzed and modeled axial cutting force, delamination effect, and surface roughness in helical milling. Brinksmeier et al. [17] described mathematically the relationship amongst bore diameter, tool diameter, and gradient of helical course, determining fundamental and qualitative statements about the cutting process of orbital drilling. Boudelier et al. [18] presented a cutting force model for machining CFRP laminate with diamond abrasive cutters and discussed the cutting mechanisms for different fibers orientation. Karpat et al. [19] developed the double helix end mill design specially for machining CFRP, and proposed a mechanistic force model for optimizing the cutting parameters. Voss et al. [20] compared the conventional

and orbital drilling of CFRP material, in terms of workpiece damage, tool wear, bore diameter variances, and cycle times.

In summary, the scholars have done a lot of relevant researches on the machining and helical milling process of CFRP material, and tool design and manufacture, mainly focusing on the microscopic analysis of machining CFRP and cutting mechanisms of hole making by helical milling [21], hole making quality [22–24], optimization of cutter angle [25, 26], grinding, etc. Bi-directional helical milling has been initially used to machine CFRP, not only prolonging the service life of cutters, but also better inhibiting burrs formation at the outlet and delamination defects [27]. However, the forward and backward milling uses respectively the top and bottom cutting zones of cutters, causing a significant difference in machining states. This makes enormous demands on the tool design, so helical milling cutters obviously cannot meet bi-directional machining need. Therefore, this paper has carried out the research into the design and manufacture of stepped bi-directional milling cutters and their cutting performance, based on the characteristics of backward helical milling in bi-directional helical milling of CFRP.

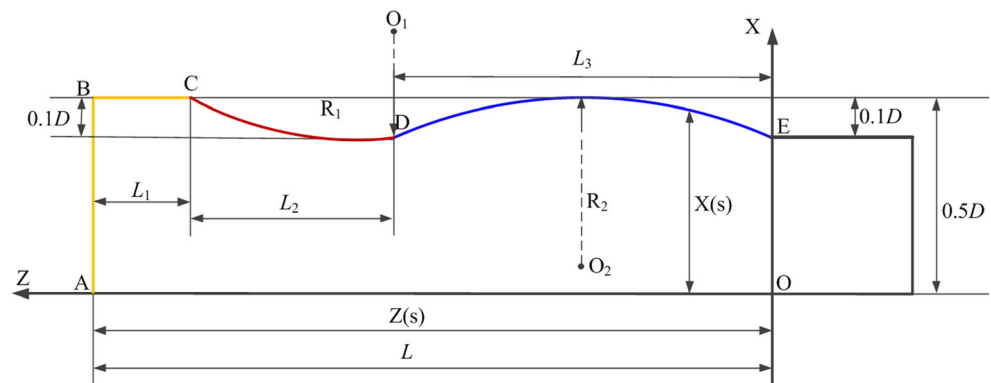
2 Design for the stepped bi-directional milling cutter

2.1 Establishing a geometric model of the stepped bi-directional milling cutter

Figure 1 shows the generatrix of the stepped bi-directional milling cutter in the plane coordinate system XOZ . The generatrix consists of the forward cutting edge zone L_1 (BC segment), the transitional cutting edge zone L_2 (CD segment) with the radius R_1 being D , and the backward cutting edge zone L_3 (DE segment) with the radius R_2 being $5D$. Therein, the tool diameter is D and the total length of the cutting edge is L . L_1 is $0.1L$ long, L_2 is $0.3L$ long, and L_3 is $0.1D$ deep.

The generatrix equation of the forward cutting edge zone L_1 is as follows:

Fig. 1 The generatrix of the stepped bi-directional milling cutter



$$\begin{cases} x(s) = 0.5D \\ z(s) = L-s \end{cases} \tag{1}$$

In the above equation, s stands for the arc length from the starting point B to any point on the circumferential cutting edge’s generatrix, and its value range is $0 \leq s \leq 0.1L$.

The generatrix equation of the transitional cutting edge zone L_2 is as follows:

$$\begin{aligned} x(s) &= D(1.4-C[(\lambda_1-s + 0.1L)/D]) \\ z(s) &= 0.6L + DS[(\lambda_1-s + 0.1L)/D] \end{aligned} \tag{2}$$

In the above equation, the value of s ranges as follows: $0.1L \leq s \leq 0.1L + \lambda_1$, $\lambda_1 = R_1 \arcsin(3L/10R_1)$, where S stands for sin and C stands for cos.

The generatrix equation of the backward cutting edge zone L_3 is as follows:

$$\begin{aligned} x(s) &= D(5C[(\lambda_1 + \lambda_2 + 0.1L-s)/5D]-4.5) \\ z(s) &= 0.3L + 5DS[(\lambda_1 + \lambda_2 + 0.1L-s)/5D] \end{aligned} \tag{3}$$

In the above equation, the value of s ranges as follows: $0.1L + \lambda_1 \leq s \leq 0.1L + \lambda_1 + \lambda_2$, $0.1L + \lambda_1 + \lambda_2 \leq s \leq 0.1L + \lambda_1 + 2\lambda_2$, and $\lambda_2 = R_2 \arcsin(3L/10R_2)$.

Figure 2 shows the gyration profile of the stepped bi-directional milling cutter in the coordinate system $O_0(X_0, Y_0, Z_0)$, the axis Z acts as the revolution axis of the tool. The equation is as follows:

$$r_m = \begin{bmatrix} x(s)C(\varphi) \\ x(s)S(\varphi) \\ z(s) \\ 1 \end{bmatrix} \tag{4}$$

In the above equation, φ stands for the angle revolving around the axis Z .

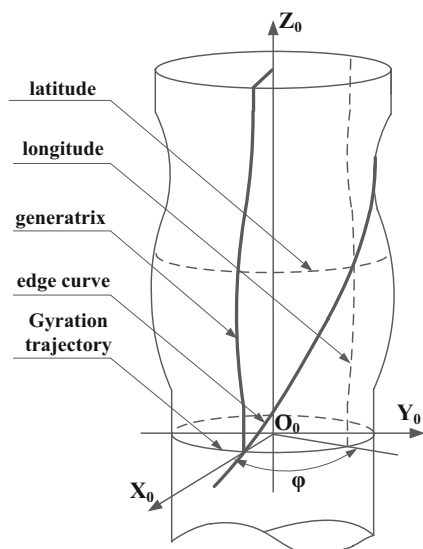


Fig. 2 The gyration profile of the stepped bi-directional milling cutter

Put Eqs. (1), (2), and (3) into Eq. (4), the gyration profile equation of the stepped bi-directional milling cutter can be derived.

The gyration profile equation corresponding to the forward cutting edge zone L_1 is as follows:

$$r_{mBC} = \begin{bmatrix} x(s)C(\varphi) \\ x(s)S(\varphi) \\ z(s) \\ 1 \end{bmatrix} = \begin{bmatrix} 0.5DC(\varphi) \\ 0.5DS(\varphi) \\ L-s \\ 1 \end{bmatrix} \tag{5}$$

The gyration profile equation corresponding to the transitional cutting edge zone L_2 is as follows:

$$r_{mCD} = \begin{bmatrix} D(0.5-C[(\lambda_1-s + 0.1L)/D])C(\varphi) \\ D(0.5-C[(\lambda_1-s + 0.1L)/D])S(\varphi) \\ 0.6L + DS[(\lambda_1-s + 0.1L)/D] \\ 1 \end{bmatrix} \tag{6}$$

The gyration profile equation corresponding to the backward cutting edge zone L_3 is as follows:

$$r_{mDE} = \begin{bmatrix} D(5C[(\lambda_1 + \lambda_2 + 0.1L-s)/5D]-4.5)C(\varphi) \\ D(5C[(\lambda_1 + \lambda_2 + 0.1L-s)/5D]-4.5)S(\varphi) \\ 0.3L + 5DS[(\lambda_1 + \lambda_2 + 0.1L-s)/5D] \\ 1 \end{bmatrix} \tag{7}$$

2.2 Modeling and simulating the edge curve of the stepped bi-directional milling cutter

As shown in Fig. 3, the edge curve of the stepped bi-directional milling cutter adopts the orthogonal helical edge curve (i.e., equal pitch edge curve). After the whole edge curve is decomposed by the differential elements, any differential element can be expressed by the increment dr . dr can be decomposed into the tangent vector $d\tau_m$ in the longitudinal direction and the normal vector $d\sigma_m$ in the latitudinal direction.

The differential increment dr of the edge curve of the stepped bi-directional milling cutter is expressed as

$$dr = d\tau_m + d\delta_m = \frac{\partial r_m}{\partial s} ds + \frac{\partial r_m}{\partial \varphi} d\varphi = \begin{bmatrix} x'(s)C\varphi ds - x(s)S\varphi d\varphi \\ x'(s)C\varphi ds + x(s)C\varphi d\varphi \\ z'(s)ds \\ 0 \end{bmatrix} \tag{8}$$

The relation between the pitch p and the angle φ is as follows:

$$d\varphi = \left[\left(\sqrt{(x')^2 + (z')^2} \right) / p \right] ds \tag{9}$$

After solving Eq. (9), put it respectively into Eqs. (5), (6), and (7), deriving the equal pitch edge curve equation of the stepped bi-directional milling cutter.

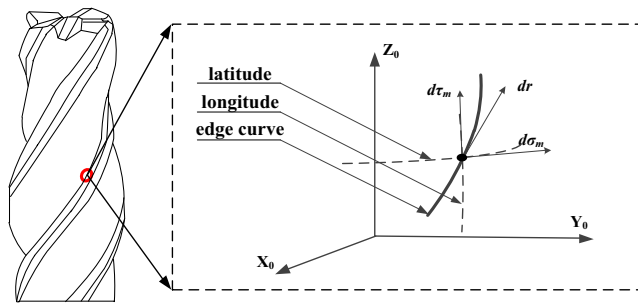


Fig. 3 Any point of the edge curve decomposed in the longitudinal and latitudinal directions

The edge curve equation corresponding to the forward cutting edge zone L_1 is as follows:

$$r_{BC} = \begin{bmatrix} x(s)C(\varphi) \\ x(s)S(\varphi) \\ z(s) \\ 1 \end{bmatrix} = \begin{bmatrix} 0.5DC(s/p) \\ 0.5DS(s/p) \\ L-s \\ 1 \end{bmatrix} \quad (10)$$

The edge curve equation corresponding to the transitional cutting edge zone L_2 is as follows:

$$r_{CD} = \begin{bmatrix} D(1.4-C[(\lambda_1-s + 0.1L)/D])C(s/p) \\ D(1.4-C[(\lambda_1-s + 0.1L)/D])S(s/p) \\ 0.6L + DS[(\lambda_1-s + 0.1L)/D] \\ 1 \end{bmatrix} \quad (11)$$

The edge curve equation corresponding to the backward cutting edge zone L_3 is as follows:

$$r_{DE} = \begin{bmatrix} D(5C[(\lambda_1 + \lambda_2 + 0.1L-s)/5D]-4.5)C(s/p) \\ D(5C[(\lambda_1 + \lambda_2 + 0.1L-s)/5D]-4.5)S(s/p) \\ 0.3L + 5DS[(\lambda_1 + \lambda_2 + 0.1L-s)/5D] \\ 1 \end{bmatrix} \quad (12)$$

Figure 4 shows the Matlab numerical simulation of the equal pitch edge curve of the four-edge stepped bi-

directional milling cutter, the tool radius being 5 mm. Figure 4 a shows the edge curve with the pitch being 25 mm, Fig. 4 b being 20 mm, and Fig. 4 c being 15 mm. As can be seen from Fig. 4, when different lead values are taken for simulation, the helical angle of the edge curve will change significantly. That is, the helical angle of the edge curve will decrease with increase of the lead value, and the simulation result conforms to the theoretical assumption.

3 Manufacture and measurement of the stepped bi-directional milling cutter

3.1 Establishing the grinding model

In order to establish the mathematical model of grinding tracks of the stepped bi-directional milling cutter, the grinding wheel coordinates of any point need converting to the workpiece coordinates. Then combining the engaging condition and edge equation of the grinding wheel and workpiece, the position and posture equation of the grinding wheel is derived about the stepped bi-directional milling cutter. As shown in Fig. 5, the transformation from the grinding wheel coordinates to workpiece coordinates in any position is based on the transformation from three translational movements of $a_x, a_y,$ and a_z to three rotational movements of $\varphi_x, \varphi_y,$ and φ_z .

The transformation matrix from the grinding wheel coordinates to workpiece coordinates is as follows:

$$\begin{aligned} & Rot(z, \varphi) Trans(a_x, a_y, a_z) RPY(\varphi_x, \varphi_y, \varphi_z) \\ &= \begin{bmatrix} \Delta_1 C\varphi_y & \Delta_1 S\varphi_y S\varphi_x - \Delta_2 C\varphi_x & \Delta_1 S\varphi_y C\varphi_x + \Delta_2 S\varphi_x & axC\varphi - ayS\varphi \\ \Delta_2 C\varphi_y & \Delta_1 S\varphi_y S\varphi_x + \Delta_1 C\varphi_x & \Delta_2 S\varphi_y C\varphi_x - \Delta_1 S\varphi_x & axS\varphi + ayC\varphi \\ -S\varphi_y & C\varphi_z S\varphi_x & C\varphi_z C\varphi_x & az \\ 0 & 0 & 0 & 1 \end{bmatrix} \quad (13) \end{aligned}$$

In the above equation, $\Delta_1 = C(\varphi + \varphi_z), \Delta_2 = S(\varphi + \varphi_z)$.

Because the transitional cutting edge zone of the stepped bi-directional milling cutter is a typical concave surface,

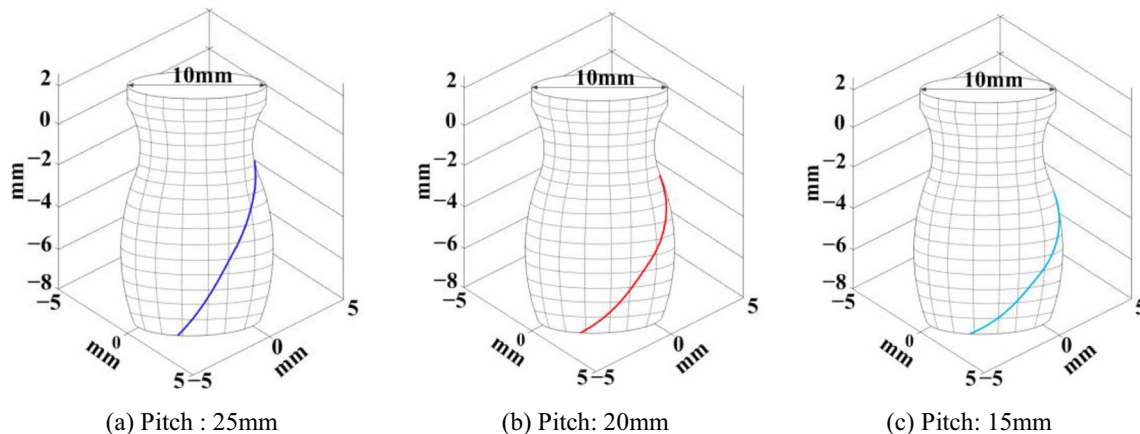
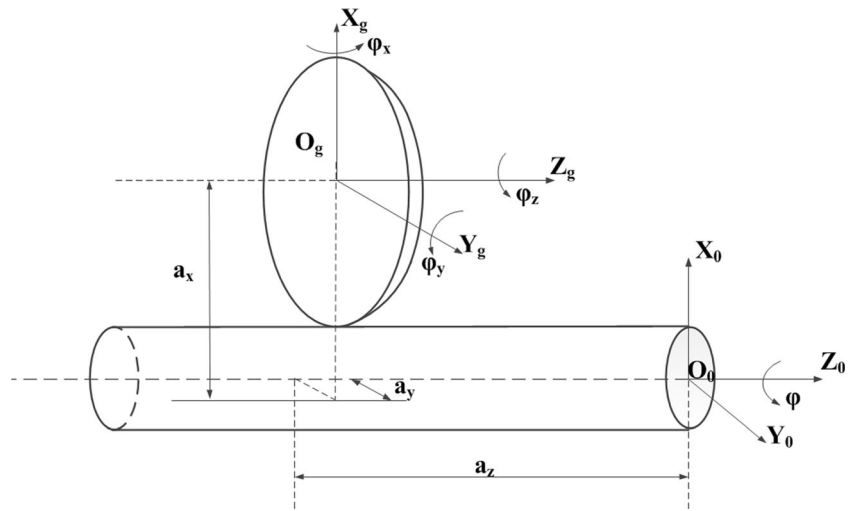


Fig. 4 Simulation of the equal pitch edge curve of the stepped bi-directional milling cutter. a Pitch 25 mm. b Pitch 20 mm. c Pitch 15 mm

Fig. 5 Transformation of grinding wheel coordinates



overcutting happens readily in course of grinding. Therefore, the segmental method is used to grind the milling cutter. The helical groove grinding area of the milling cutter is segmented as shown in Fig. 6.

In Fig.6, the helical groove grinding area is divided into three parts. The first part is the forward zone, the second is the transitional zone, and the third is the backward zone. The grinding process consists of two stages. The first one is to grind the forward zone, while the second is to grind the backward zone. Therein, the transitional zone is employed to guarantee grinding accuracy and continuity of the forward and backward zones.

The grinding wheel track equation in the workpiece coordinates is as follows:

$$G = \text{Rot}(z, \varphi) \text{Trans}(a_x, a_y, a_z) \text{RPY}(\varphi_x, \varphi_y, \varphi_z) r_{DE} \quad (14)$$

Put Eqs. 12 and 13 into Eq. 14, and then the grinding wheel track equation in the workpiece coordinates is derived during grinding the helical groove in the backward zone. It is as follows:

$$G_{DE} = \begin{bmatrix} \Delta_1 [\Delta_3 C(s/p)C\varphi_y + \Delta_3 S(s/p)S\varphi_y S\varphi_x + \Delta_4 S\varphi_y C\varphi_x] + \Delta_2 [\Delta_3 S(s/p)C\varphi_x + \Delta_4 S\varphi_x] + a_x C\varphi - a_y S\varphi \\ \Delta_2 [\Delta_3 C(s/p)C\varphi_y + \Delta_3 S(s/p)S\varphi_y S\varphi_x + \Delta_4 S\varphi_y C\varphi_x] + \Delta_1 [\Delta_3 S(s/p)C\varphi_x - \Delta_4 S\varphi_x] + a_x S\varphi + a_y C\varphi \\ \Delta_3 [S(s/p)C\varphi_z S\varphi_x - C(s/p)S\varphi_y] + \Delta_4 C\varphi_z C\varphi_x + a_z \\ 1 \end{bmatrix} \quad (15)$$

In the above equation, $\Delta_3 = D[1.5 - S(s/D)]$, $\Delta_4 = 0.1L + DC(s/D)$.

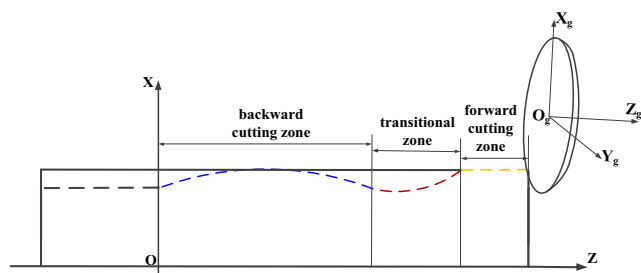


Fig. 6 Helical groove grinding area of the stepped bi-directional milling cutter

3.2 Manufacture and measurement of the stepped bi-directional milling cutter

The stepped bi-directional milling cutter is ground on the five-axis grinding center SAACKE UWI, the original rod is the hard alloy rod YG8 from JINLU company, and the accuracy is measured on ZOLLER G3. The grinding site and measurement of geometric angles are shown in Fig. 7. The measuring accuracy meets the following demand. That is, in Fig. 7 b, the rake angle is in the range of $1 \pm 0.05^\circ$, the first flank angle is $8 \pm 0.05^\circ$, the second flank angle is $16 \pm 0.05^\circ$, and the helical angel is $35 \pm 0.05^\circ$. After the above measurement, the tool is

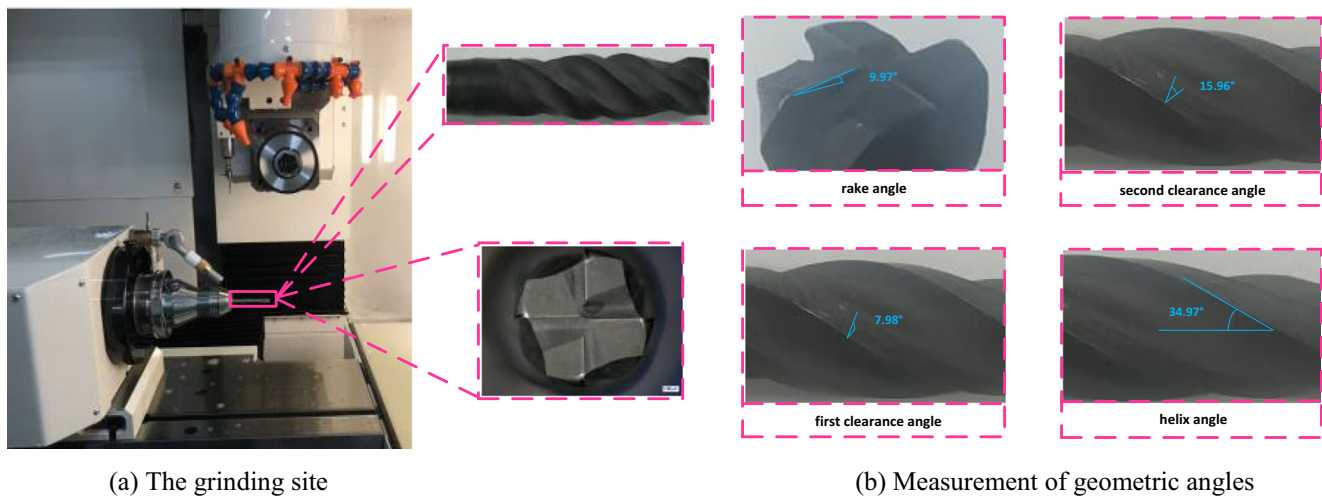


Fig. 7 Grinding results of the stepped bi-directional milling cutter. **a** The grinding site. **b** Measurement of geometric angles

coated with the multi-layer diamond composite, and the coating is 10- μm thick.

Figure 8 a shows the detection site, where ZOLLER G3 is used to measure the geometric profile accuracy of the machined stepped bi-directional milling cutter, and the measuring results are shown in Fig. 8 b. In the figure, the red lines represent the theoretical geometric profiles, and the blue lines represent the tolerance zone. It can be learned from the measuring results of grinding accuracy that the grinding accuracy of geometric profiles of both forward and backward edge zones meets the demand. Nevertheless, there is a minor out-of-tolerance of the geometric profile next to the concave arc bottom in the transitional zone. Considering the transitional zone is not involved in the cutting, the out-of-tolerance will not affect the cutter performance.

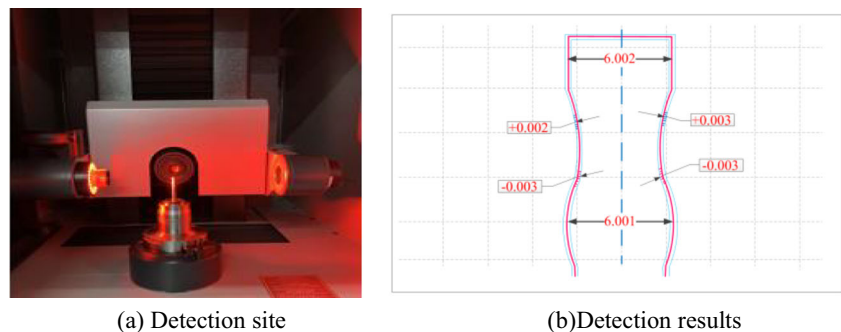
4 Comparative experiment of the bi-directional helical milling using two different milling cutters

4.1 Experimental design

In order to evaluate the cutting performance of stepped bi-directional milling cutters, this paper has designed the

comparative experiment of milling CFRP using the stepped bi-directional helical milling cutters and symmetrical bi-directional helical milling cutters. The experiment site is shown in Fig. 9 a. The experiment is carried out on the three-axis milling center VDL-1000E, and the cutters for the experiment, as shown in Fig. 9 b, are self-made bi-directional milling cutters, respectively, stepped and symmetrical. The two types of cutters are the same in the other geometric parameters but in the geometric profiles. Namely, the diameters are 6 mm, the helical angles are 35°, the rake angles are 10°, and the flank angles are 8°. The multi-directional laid CFRP composite is selected as the experimental material. Its matrix material is AG80 epoxy resin, and its reinforcing material is T700 fiber bundles. For the fiber bundles, its fiber volume ratio is $60 \pm 5\%$, and for the CFRP composite, it is 200-mm long, 110-mm wide, and 6-mm thick. The bi-directional helical milling process is adopted in the experiment as shown in Fig. 9 c. The milling process consists of two stages, forward and backward. In the first stage, the eccentricity is set as 1 mm, and the milling proceeds forward until the hole reaches 4-mm deep. Then, the eccentricity is decreased to 0.8 mm, the milling continues until the whole hole is made through. In the second stage, the eccentricity is adjusted back to 1 mm, but the milling proceeds backward and removes the reserved machining allowance until the through-hole with a diameter of

Fig. 8 The detection results of grinding accuracy. **a** Detection site. **b** Detection results



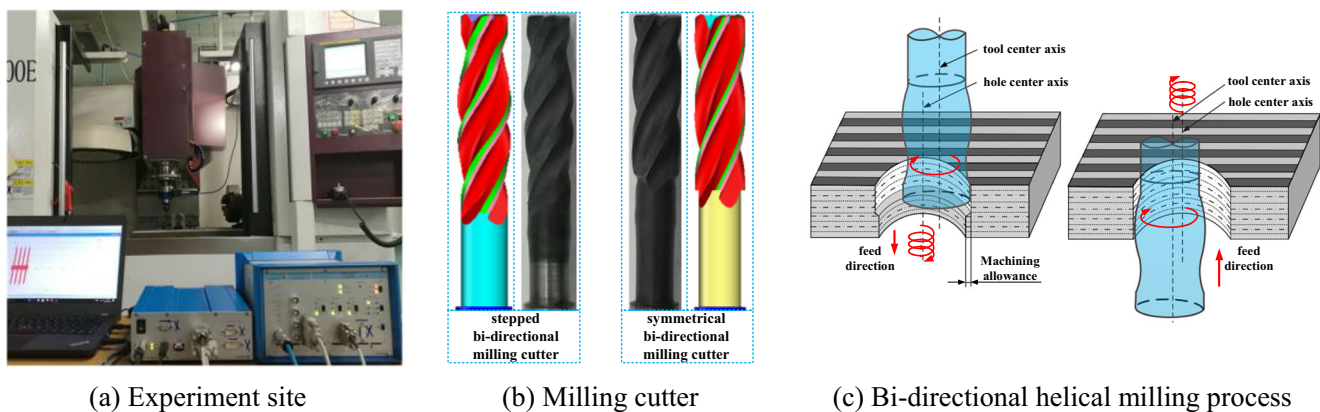


Fig. 9 The experiment site and bi-directional helical milling process. **a** Experiment site. **b** Milling cutter. **c** Bi-directional helical milling process

8 mm is machined through. In the experiment, the cutting parameters keep invariable as shown in Table 1.

In the experiment, the Kister 9171A rotary dynamometer is used to collect the cutting force data. Every 5 milling holes are machined through before the cutter is removed. And then, a VHX-1000 super-high magnification zoom lens microscope and SU3500 scanning electron microscope are used to detect the wear macro-morphology and micro-morphology of forward and backward cutting edges. After the experiment finishes, the workpiece is removed, and then the VHX-1000 super-high magnification zoom lens microscope is used to further observe the machining morphology in the inlet and outlet area of the hole making, and the TR200 measuring instrument is used to measure the hole wall roughness Ra .

4.2 Analysis of the cutting forces

Figure 10 shows the cutting forces produced by milling CFRP backward with the symmetrical structure and stepped structure bi-directional milling cutters, the rotary speed of the main spindle being 4500 r/min, the feed per tooth being 0.03 mm/z, and the machining pitch being 0.2 mm. It can be seen from the figure that for the two milling cutters, the tangential force F_x and the radial force F_y are both larger than the axial force F_z . In contrast, the stepped bi-directional milling cutter has larger F_x and F_y , but smaller F_z than the symmetrical bi-directional milling cutter, because a gradual helical angle forms on the backward cutting edge of the stepped bi-directional cutter along the arc profile, effectively

decomposing part of the axial force. In addition, compared with the symmetrical bi-directional milling cutter, the stepped bi-directional milling cutter shows more gentle fluctuation of the axial force F_z , because the latter has longer cutting edge than the former involved in the backward machining, effectively reducing the influence of the frictional resistance and mechanical impact, and improving the machining stability.

Figure 11 shows the comparison of cutting forces produced by milling CFRP backward with the symmetrical structure and stepped structure bi-directional milling cutters in the condition of different numbers of holes. As the number of holes rises, all the cutting forces produced by the stepped bi-directional milling cutter increase more slowly than the symmetrical bi-directional milling cutter, because while machining backward with the former, the gradual helical edge effectively lengthens the contact edge in the cutting zone, making the tool wear slow down.

4.3 Analysis of the tool wear

Figure 12 shows the comparison of the tool wear morphology in milling CFRP backward with the symmetrical structure and stepped structure bi-directional milling cutters. As can be seen from Fig. 12 a, when finishing making 30 holes, for both types of milling cutters, the spoon-shaped wear band forms on the flank surface of the forward cutting edge, and strip-shaped wear band occurs on the flank surface of the backward cutting edge. In contrast, as shown in Fig. 12 b, there is a little larger area of spoon-shaped wear band on the flank surface of the

Table 1 The cutting parameters used in the tests

Cutting parameter tool	Spindle speed (4500 rpm/min)	Feed per tooth (mm/tooth)	Pitch (mm)
Symmetrical bi-directional milling cutter	4500	0.03	0.2
Stepped bi-directional milling cutter	4500	0.03	0.2

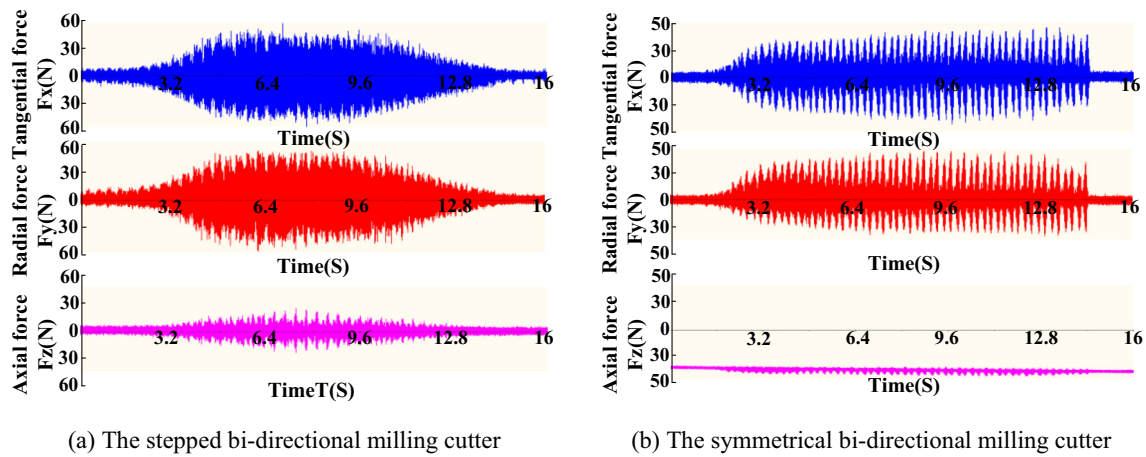


Fig.10 The cutting forces produced by milling CFRP backward with the two types of milling cutters

Fig. 10 The cutting forces produced by milling CFRP backward with the two types of milling cutters. **a** The stepped bi-directional milling cutter. **b** The symmetrical bi-directional milling cutter

forward cutting edge of the stepped bi-directional milling cutter. As more and more holes are made, the tool wear develops more and more seriously. When finishing making 80 holes, for both types of milling cutters, fairly large areas of spoon-shaped and strip-shaped wear bands occur respectively on the flank surfaces of their forward and backward cutting edges, and a lot of notches appear on the cutting edges. It is found by comparing the wear morphology on the forward and backward cutting edges of the two types of milling cutters that the tool wear differs slightly on the forward cutting edges of the two milling cutters. However, on the backward cutting edges, the symmetrical bi-directional milling cutter shows more serious and concentrative wear. That is mainly because in the backward machining with the stepped bi-directional milling cutter, the effect of the gradual helical edge increases the cooling space and decreases the cutting force fluctuation, greatly improving the thermodynamic load between the tool and workpiece.

4.4 Analysis of hole making quality

Figure 13 shows the comparison of the inlet and outlet machining quality of the 30th and the 80th holes made by the stepped structure and symmetrical structure bi-directional milling cutters. When milling the 30th hole, for both types of milling cutters, the inlet surface quality of the hole is fairly ideal because of no defects such as burrs and tearing. While milling the 80th hole, a small number of burrs appear at the inlet of the holes made by the two milling cutters, but the difference of processing quality at the exit is not obvious.

However, there are obvious differences of machining quality at the outlet of the holes. When milling the 30th hole, a small number of burrs and slight tearing appear at the outlet of the hole made by the symmetrical bi-directional milling cutter, while the outlet of the hole made by the stepped bi-directional milling cutter still keeps smooth. As the machining proceeds, the cutting performance of tools gradually decreases; when milling the 80th hole, a lot of burrs and tearing form at the outlet of the hole made by the symmetrical bi-directional milling cutter, while only a small number of burrs occur at the outlet of the hole made by the stepped bi-directional milling cutter. At this moment, the hole wall roughness *Ra* caused by the stepped bi-directional milling cutter is 4.9 μm , and the one by the symmetrical bi-directional milling cutter even reaches 7.3 μm . This is mainly because the backward cutting edge wear of the stepped bi-directional milling cutter is relatively slight, keeping the integrity and sharpness of the cutting edge better.

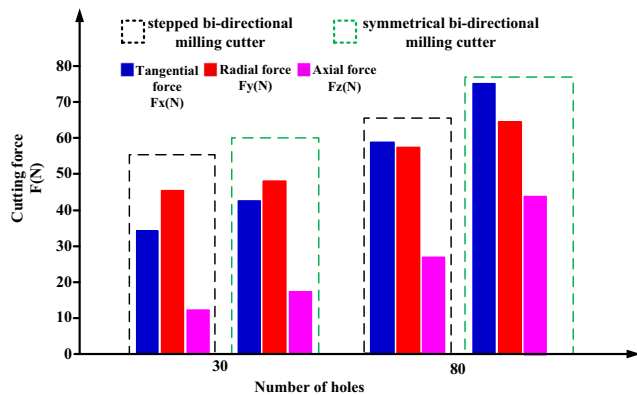
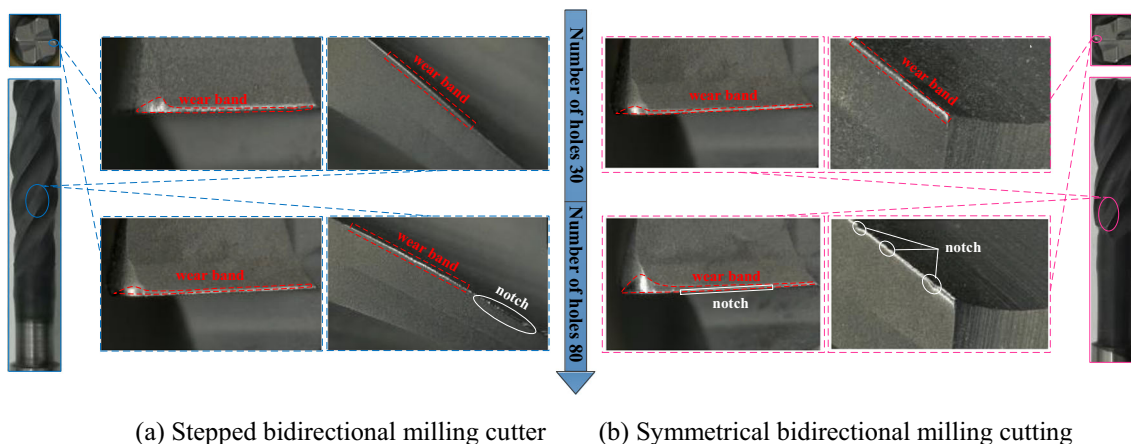


Fig. 11 Comparing the cutting forces produced by milling CFRP backward in the condition of different numbers of holes

5 Conclusions

In this paper, the mathematical model and grinding model of the stepped bi-directional milling cutter are established by



(a) Stepped bidirectional milling cutter (b) Symmetrical bidirectional milling cutting

Fig. 12 Comparison of wear morphology of the two types of milling cutters. (a) Stepped bi-directional milling cutter. (b) Symmetrical bi-directional milling cutting

using the differential geometry method. What is more, the excellent performance of the stepped bi-directional milling cutter in the two-way spiral milling of CFRP is verified by the comparative experiment. The main research results of this paper are as follows:

- (1) The design for and research on stepped bi-directional milling cutters for bi-directional helical milling are carried out, the differential geometry method is used to derive the segmental profile equation, and the mathematical model of the equal pitch helical edge curve of stepped bi-directional milling cutters is established.
- (2) The transformation matrix between grinding wheel and workpiece coordinates is deduced, the mathematical

model of helical groove grinding path of stepped bi-directional milling cutters is established, and the grinding accuracy of the stepped bi-directional milling cutter is measured, achieving the quantitative evaluation of the grinding accuracy of the developed cutters.

- (3) A comparative and experimental study on the cutting performance of stepped structure and symmetrical structure bi-directional milling cutters is carried out in the helical milling of CFRP. It is found that for the stepped bi-directional milling cutter, the axial cutting force in the backward helical milling is smaller and fluctuates more smoothly, and as the number of holes rises, all the cutting forces increase relatively slowly, making the cutting stability better.

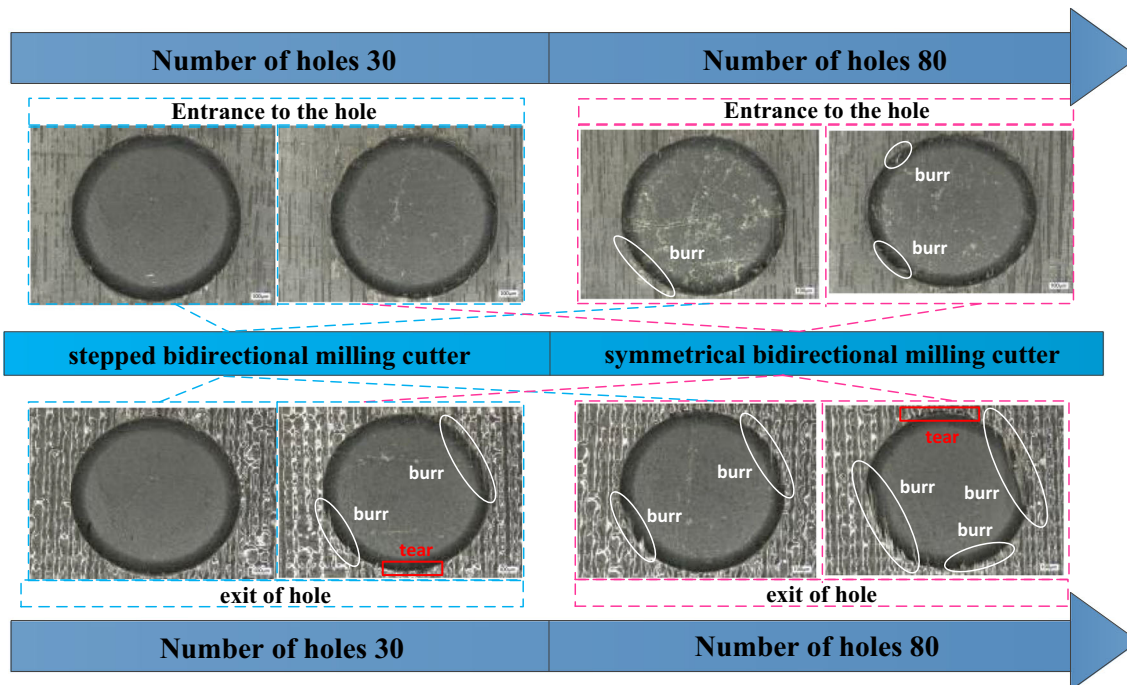


Fig. 13 Comparison of the inlet and outlet machining quality of the 30th and the 80th holes made by the two types of cutters

- (4) In contrast with the symmetrical bi-directional milling cutter, better distributed wear occurs on the backward cutting edge of the stepped bi-directional milling cutter, and the strip-shaped wear band is long and narrow. Moreover, with aggravation of the tool wear, no obvious concentrative wear appears, and the hole making quality is relatively better.

Funding information The authors would like to acknowledge the support of the National Natural Science Foundation of China (Grant No.51975168).

Compliance with ethical standards

Conflict of interest The authors declare that they have no conflict of interest.

References

- Robson BD, Dutra P, Lincoln CB, Anderson PP, João RF, Paulo DJ (2017) A review of helical milling process. *Int J Mach Tools Manuf* 120(5):27–48
- Yang GL, Dong ZG, Kang RK, Bao Y, Guo DM (2019) Research progress of helical milling. *Acta Aeronautica et Astronautica Sinica* 40(X):1–17 (in Chinese).
- Wang Q, Wu YB, Bitou T, Mitsuyoshi N, Tatauya F (2018) Proposal of a tilted helical milling technique for high quality hole drilling of CFRP: kinetic analysis of hole formation and material removal. *Int J Adv Manuf Technol* 94(9–12):4221–4235
- Zhou L, Dong H, Ke Y, Cheng GL (2016) Analysis of the chip-splitting performance of a dedicated cutting tool in dry orbital drilling process. *Int J Adv Manuf Technol* 90(5–8):1–15
- Liu G, Wang YF, Zhang H, Gao KY, Ke YL, Duan ZH (2014) Research on helical milling specialized tool based on chip-splitting principle. *Journal of Mechanical Engineering* 50(9):176–184 (in Chinese).
- Chen XF, Ding GF, Li R, Ma XJ, Qin SF, Song XL (2014) A new design and grinding algorithm for ball-end milling cutter with tooth offset center. *J Eng Manuf* 228(7):687–697
- Tian YL, Liu YP, Wang FJ, Jing XB, Zhang DW, Liu XP (2017) Modeling and analyses of helical milling process. *Int J Adv Manuf Technol* 90(1–4):1003–1022
- Ren L, Wang SL, Yi LL, Sun SL (2015) An accurate method for five-axis flute grinding in cylindrical end-mills using standard 1V1/1A1 grinding wheels. *Precis Eng* 43(9):387–394
- Wang LL, Chen ZC, Li JF, Sun J (2016) A novel approach to determination of wheel position and orientation for five-axis CNC flute grinding of end mills. *Int J Adv Manuf Technol* 84(9–12):2499–2514
- Nguyen H, Ko SL (2014) A mathematical model for simulating and manufacturing ball end mill. *Comput Aided Des* 50(1):6–26
- An QL, Cai CY, Cai XJ, Chen M (2019) Experimental investigation on the cutting mechanism and surface generation in orthogonal cutting of UD-CFRP laminates. *Compos Struct* 230:111441
- Gökhan S, Ömer E (2018) Cutting tool geometry in the drilling of CFRP composite plates and Taguchi optimisation of the cutting parameters affecting delamination. *Sigma Journal of Engineering and Natural Sciences Sigma Mühendislik ve Fen Bilimleri Dergisi* 36(3):619–628
- Ömer E, Birhan I, Adem Ç, Fuat K (2013) Prediction of damage factor in end milling of glass fibre reinforced plastic composites using artificial neural network. *Appl Compos Mater* 20(4):517–536
- Qi Z, Zhang K, Cheng H, Liu S (2015) Numerical simulation for delamination during drilling of CFRP/AL stacks. *Mater Res Innov* 19(Sup6):98–101
- Ventura CEH, Hassui A (2013) Modeling of cutting forces in helical milling by analysis of tool contact angle and respective depths of cut. *Int J Adv Manuf Technol* 68(9):2311–2319
- Norbert G, Tibor S (2017) Optimisation of process parameters for the orbital and conventional drilling of unidirectional carbon fibre-reinforced polymers (UD-CFRP). *Measurement* 110(7):319–334
- Brinksmeier E, Fangmann S, Meyer I (2008) Orbital drilling kinematics. *Prod Eng* 2(3):277–283
- Boudelier A, Ritou M, Garnier S, Furet B (2018) Cutting force model for machining of CFRP laminate with diamond abrasive cutter. *Prod Eng* 12(2):279–287
- Karpat Y, Polat N (2013) Mechanistic force modeling for milling of carbon fiber reinforced polymers with double helix tools. *CIRP Ann-Manuf Technol* 62(1):95–98
- Voss R, Henerichs M, Kuster F (2016) Comparison of conventional drilling and orbital drilling in machining carbon fibre reinforced plastics (CFRP). *CIRP Ann-Manuf Technol* 65(1):137–140
- Li ZQ, Liu Q, Ming XZ, Dong YF (2014) Cutting force prediction and analytical solution of regenerative chatter stability for helical milling operation. *Int J Adv Manuf Technol* 73(1–4):433–442
- Li ZQ, Liu Q (2013) Surface topography and roughness in hole-making by helical milling. *Int J Adv Manuf Technol* 66(9–12):1415–1425
- Shang YC, He N, Li L, Zhao W, Yang YF (2013) Vector modeling of robotic helical milling hole movement and theoretical analysis on roughness of hole surface. *J Cent South Univ* 20(7):1818–1824
- An QL, Chen J, Cai XJ, Peng TT, Chen M (2018) Thermal characteristics of unidirectional carbon fiber reinforced polymer laminates during orthogonal cutting. *J Reinf Plast Compos* 37(13):905–916
- Ömer E, Mustafa D, Birhan I, İbrahim NT (2014) Selection of optimal machining conditions for the composite materials by using Taguchi and GONNs. *Measurement* 48:306–313
- Chen Y, Ge ND, Fu YC, Su HU, Xu JH (2015) Review and prospect of drilling technologies for carbon fiber reinforced. *Acta Materiae Compositae Sinica* 32(2):301–314 (in Chinese)
- Dong HY, Chen GL, Zhou L, He FT, Liu ST (2017) Processing research on orbital drilling of CFRP/Ti-6Al-4V stacks. *Acta Materiae Compositae Sinica* 34(3):540–549 (in Chinese)

Publisher's note Springer Nature remains neutral with regard to jurisdictional claims in published maps and institutional affiliations.